Scarring of Dirac fermions in chaotic billiards

Xuan Ni,[1] Liang Huang,[1,2] Ying-Cheng Lai,[1,3,4] and Celso Grebogi[4]

[1]*School of Electrical, Computer and Energy Engineering, Arizona State University, Tempe, Arizona 85287, USA*

[2]*Institute of Computational Physics and Complex Systems, and Key Laboratory for Magnetism and Magnetic Materials of MOE, Lanzhou University, Lanzhou, Gansu 730000, China*

[3]*Department of Physics, Arizona State University, Tempe, Arizona 85287, USA*

[4]*Institute for Complex Systems and Mathematical Biology, King's College, University of Aberdeen, Aberdeen AB24 3UE, United Kingdom*

Scarring in quantum systems with classical chaotic dynamics is one of the most remarkable phenomena in modern physics. Previous works were concerned mostly with nonrelativistic quantum systems described by the Schrödinger equation. The question remains outstanding of whether *truly* relativistic quantum particles that obey the Dirac equation can scar. A significant challenge is the lack of a general method for solving the Dirac equation in closed domains of arbitrary shape. In this paper, we develop a numerical framework for obtaining complete eigensolutions of massless fermions in general two-dimensional confining geometries. The key ingredients of our method are the proper handling of the boundary conditions and an efficient discretization scheme that casts the original equation in a matrix representation. The method is validated by (1) comparing the numerical solutions to analytic results for a geometrically simple confinement and (2) verifying that the calculated energy level-spacing statistics of integrable and chaotic geometries agree with the known results. Solutions of the Dirac equation in a number of representative chaotic geometries establish firmly the existence of scarring of Dirac fermions.

I. INTRODUCTION

Given a closed Hamiltonian system that exhibits fully developed chaos in the classical limit, one might expect the quantum wave functions associated with various eigenstates to be more or less uniform in the physical space. This had been thought to be quite natural because of ergodicity associated with chaos in the classical phase space. The notion of uniform wave functions was nevertheless proven to be wrong about three decades ago, when strongly nonuniform eigenfunctions were discovered by McDonald and Kaufman in their study of the eigensolutions of the Schrödinger equation in the chaotic stadium billiard [1]. A systematic study was subsequently carried out by Heller [2], who established the striking tendency for wave functions to concentrate about classical unstable periodic orbits, which he named *quantum scars*. Semiclassical theory was then developed by Bogomolny [3] and Berry [4], providing a general understanding of the physical mechanism of quantum scars. It should be noted that the phenomenon was deemed counterintuitive and surprising solely because of *chaos*, as the phase space of an integrable system is not ergodic so the quantum wave functions are generally not expected to be uniform. Quantum scars are one of the most remarkable phenomena in modern physics and have become an active area of research [5].

Existing works on scarring so far have focused on the nonrelativistic quantum regime governed by the Schrödinger equation. A fundamental issue is whether, in a closed chaotic billiard, relativistic quantum particles obeying the Dirac equation can scar. This issue was partially addressed in the context of closed graphene [6] confinements, where signatures of quantum scars were identified in the patterns of the local density of states [7]. The framework used in the study, however, was based on tight-binding Hamiltonian and nonequilibrium Green's function derived still from the Schrödinger equation.

The question of whether truly Dirac fermions, particles strictly obeying the Dirac equation, can scar in chaotic billiards has not been addressed.

In fact, a general method for completely solving the Dirac equation in *closed* system of *arbitrary* geometry did not exist. The main reason is that, although the Dirac equation is the cornerstone of relativistic quantum mechanics and quantum electrodynamics, solutions were focused on free space and perturbation types in situations where relativistic quantum behaviors occur. Prior to the discoveries of graphene and topological insulators [8], it was not generally thought that relativistic quantum mechanics would practically be relevant to solid-state devices. As a result, there was little interest in studying the Dirac equation in *finite domains*. The only exception was the work of Berry and Mondragon [9], who in 1987 developed a boundary-integral type of method to solve the energy levels (eigenvalues) of a chaotic neutrino billiard. To obtain the eigenfunctions, a closed form of the boundary of the domain is needed. To our knowledge, for closed domains of *arbitrary* shapes, a general method for obtaining *both* the eigenvalues and eigenstates of Dirac fermions did not exist [10].

A number of areas in physics can benefit enormously from an efficient method for solving the Dirac equation. The most relevant area is graphene physics. Graphene ribbons exhibit a linear energy-momentum relation near any of the Dirac points in the energy-band diagram, which is a characteristic of relativistic quantum motion of massless fermions. In the presence of short-range potentials, two Dirac points are coupled together. It is, thus, of basic interest to investigate the behavior of pure Dirac fermions to distinguish them from those due to the coupling of two relativistic particles. In a recent work [10], a method was developed to study the effect of Dirac fermions in graphene employing the transfer-matrix technique, which addresses the transport properties

of a graphene ribbon with periodic boundary conditions in the transverse direction. However, most existing works on quantum transport properties of graphene systems were carried out in, for example, the tight-binding Hamiltonian framework derived from the nonrelativistic Schrödinger equation [11].

In this paper, we develop a general and efficient method to solve the Dirac equation for massless fermions in a two-dimensional closed system. An obstacle to obtaining a complete solution of the Dirac equation, which includes both eigenvalues and eigenfunctions, is the proper handling of the boundary conditions. We shall develop an efficient discretization scheme and a physically meaningful approach to treating the boundary conditions, based on converting the Dirac equation into a set of matrix equations. In our method, the physical symmetries of the system are well preserved. To validate our method, we consider three types of representative geometric confinements, which include domains that generate both integrable and chaotic motions in the classical limit, and calculate the complete spectrum of eigenvalues and the associated eigenvector set. In particular, in the case of integrable geometries for which analytic predictions of the eigenvalues and eigenvectors are available, we obtain excellent agreement between the numerical and analytic results. For more general geometries, including classically chaotic systems, the properties of our calculated eigenvalue spectrum, such as the energy level-spacing statistics, agree well with the known results for different symmetry classes [9]. In fact, our method is capable of finding eigenstates of Dirac fermions under arbitrarily electrical potential profiles. Our matrix formulation can be applied directly to one-dimensional systems and, by a straightforward extension of the Dirac spinor to four components and by a proper revision in the discretization and boundary constraints, the method can be extended to solving the Dirac equation in three dimensions as well. Our main finding is that the relativistic, spinor type of wave functions associated with Dirac fermions can be highly nonuniform in chaotic billiards, and truly relativistic quantum scars *do* exist.

We remark that in the earlier work of Berry and Mondragon on neutrino billiards [9], eigenvalues were computed using the boundary-integral method. However, the Green's function utilized in the boundary integral is the one associated with open systems. They showed that the higher-order correction terms of the Green's function due to boundaries do not contribute to the energy spectrum. However, for a complete solution set, where not only eigenvalues but also eigenfunctions are of interest, it is necessary to obtain the Green's function for the closed system, which is not feasible for *arbitrary* shaped domains and not necessarily smooth boundaries under the framework of boundary integrals. Consequently, one still needs an appropriate discretization scheme to solve the closed-system Dirac equation, either by numerically evaluating the Green's function or by solving the eigenvalue problem directly.

In Sec. II, we detail our method for obtaining complete solutions of the Dirac equation in two-dimensional closed systems, focusing on proper handling of boundary conditions and on the articulation of discretization scheme. In Sec. III, we test our algorithm using an idealized domain for which analytic solutions of the Dirac equation can be written down, and obtain further validation by calculating the energy

level-spacing statistics for three different types of closed geometries. Calculation of the eigenstates establishs firmly the existence of relativistic quantum scars in Dirac fermion systems. In Sec. V, we present conclusions and a discussion.

II. METHOD

A. Background

A subtle and challenging issue in solving the Dirac equation is the proper treatment of the boundary conditions [12]. Due to the finite domain and the first-order nature of the Dirac equation, a naive treatment of the boundary conditions will lead to trivial or even nonphysical solutions. One example is the relativistic particle in a one-dimensional box. By simply letting the whole spinor go to zero at the walls of the box, only a trivial (all-zero) solution of the eigenfunctions are obtained. To overcome this difficulty, many self-adjoint extensions of the boundary conditions in both Dirac and Weyl representations have been proposed [13]. For example, in $(1 + 1)$ dimensions, one family of boundary conditions is to force either the large or the small component of the spinor to be zero at the walls of the box. Some variances of these boundary conditions also exist [14,15], e.g., by assuming that the large component vanishes at one boundary and the small component vanishes at the other or by assuming that both components differ by factors $\pm i$. Some of these boundary conditions also preserve the physical symmetries, such as *P* and *CPT* symmetries. However, these types of conditions are not all appropriate in $(2 + 1)$ dimensions, because the walls of the box are impenetrable. Physically, this means that the relativistic current $\mathbf{j} = c\psi^\dagger \boldsymbol{\sigma} \psi$ normal to the boundaries must vanish. The vanishing current condition has been used in the bag model [16–18] of quark confinement, which solves the Dirac equation with a Lorentz scalar potential. It was assumed that the rest mass of the particle $m(\mathbf{r})$ is a position-dependent parameter. One could then solve this infinite-well problem for the particle of varying mass, letting the mass go to infinity outside the box in order to take into account the Klein paradox. A similar method was adopted by Berry *et al.* [9] for studying random-matrix theory and energy level-spacing statistics for relativistic neutrino billiards. We consider a two-dimensional closed system within which a relativistic, massless fermion is confined, as shown schematically in Fig. 1. The system is governed by the Dirac equation in $(2 + 1)$ dimensions,

$$i\hbar\partial_t\psi(t) = \hat{H}\psi(t), \tag{1}$$

where the general form of the Hamiltonian is given by

$$\hat{H} = c(\boldsymbol{\alpha} \cdot \mathbf{p}) + \beta mc^2 \tag{2}$$

and ψ is a two-component Dirac spinor. Assuming stationary solution $\psi(t) = \psi \exp(-iEt/\hbar)$, we obtain the steady-state Dirac equation

$$\hat{H}\psi = E\psi. \tag{3}$$

In two dimensions, $\boldsymbol{\alpha} = \boldsymbol{\sigma} = (\sigma_x, \sigma_y)$ and $\beta = \sigma_z$ are choices satisfying all anticommutation/commutation relations of Dirac/Lorentz algebra [19].

To obtain the proper boundary conditions, two methods can be employed: We either replace the $mc^2\sigma_z$ term with a potential $U(\mathbf{r})\sigma_z$ in the Hamiltonian and let $U(\mathbf{r})$ go to infinity outside
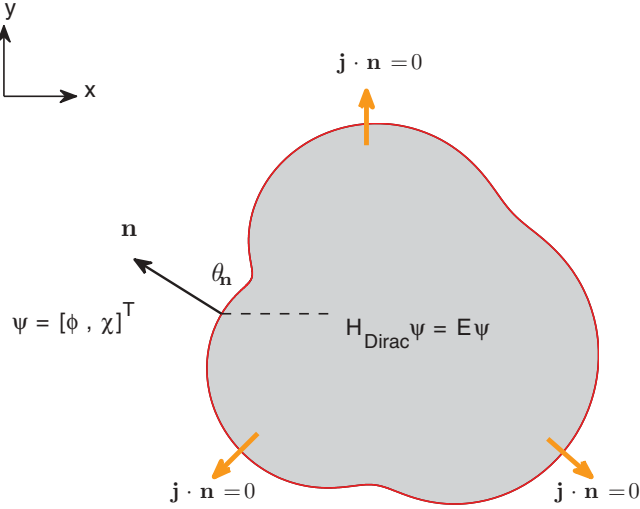
FIG. 1. (Color online) Schematic picture of closed Dirac system with arbitrary geometry and zero outgoing flux boundary condition $\mathbf{j} \cdot \mathbf{n} = 0$. This boundary condition is equivalent to $\chi/\phi = i \exp(i\theta_{\mathbf{n}})$ with $\theta_{\mathbf{n}}$ being the argument of the surface normal $\mathbf{n}$.

the domain or use the vanishing current condition $\mathbf{j} \cdot \mathbf{n} = 0$, where $\mathbf{n}$ is the boundary surface normal, as shown in Fig. 1. The latter method yields

$$\mathrm{Re}(e^{i\theta_{\mathbf{n}}}\phi/\chi) = 0,$$

where ϕ and χ are the components of the Dirac spinor, $\psi = (\phi, \chi)^T$, and $\theta_{\mathbf{n}}$ is the argument of the surface normal $\mathbf{n}$. The boundary condition can then be written as [9]

$$\chi/\phi = i \exp(i\theta_{\mathbf{n}}). \tag{4}$$

When an external electric potential energy V is present, E is replaced by $E - V$. For massless fermions, we then can write the Dirac equation as

$$[v(\boldsymbol{\sigma} \cdot \mathbf{p}) + V]\psi = E\psi, \tag{5}$$

where we replace c by v for more generalized cases or, for instance, in graphene, by the Fermi velocity $v_F \sim 10^6$ m/s.

B. Discretization scheme and elimination of fermion doubling effect

To numerically solve the Dirac equation, it is necessary to develop an efficient and physically meaningful discretization scheme. Unlike the standard discretization of second-order differential equations such as the Schrödinger equation, discretization for the massless Dirac equation is a much harder problem. An important issue is that the usual finite difference methods fail because they introduce the so-called *fermion-doubling* effect, even for open or periodic boundaries. Fermion doubling is also a problem for lattice QCD computations [16–18].

To explain the fermion-doubling phenomenon, we take the one-dimensional Dirac equation,

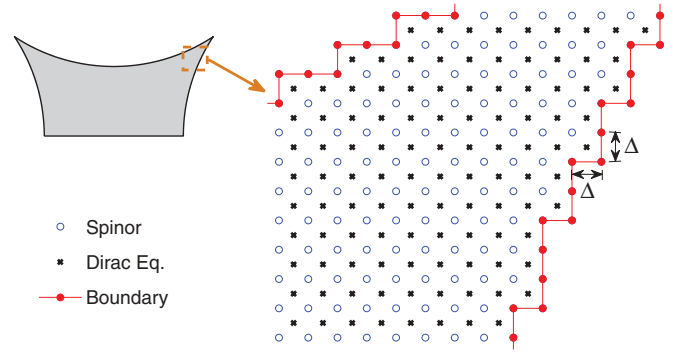$$i\hbar\partial_t\psi = i\hbar v\sigma_x\partial_x\psi, \tag{6}$$

FIG. 2. (Color online) Proposed discretization scheme to eliminate any fermion-doubling effect. A two-dimensional domain, which exhibits chaos in the classical limit, is illustrated to show the discretized lattice. Red solid circles and blue open circles spaced by Δ represent the boundary and inner lattice points, respectively, where the Dirac spinor values are sampled. The actual Dirac equations are evaluated at black cross points, the centers of unit cells.

as an example. Using the usual lattice grid $x = n\Delta$ and the central difference approximation,

$$\partial_x\psi(n) = [\psi(n+1) - \psi(n-1)]/(2\Delta),$$

the Fourier transformed equation is

$$i\hbar\partial_t\tilde{\psi} = [\hbar v\sigma_x \sin(p_x\Delta)/\Delta]\tilde{\psi} = \tilde{H}\tilde{\psi}. \tag{7}$$

We see that the energy is given by

$$|E| = |\hbar v\sigma_x \sin(p_x\Delta)/\Delta|. \tag{8}$$

In the first Brillouin zone (BZ) where $p \in [-\pi/\Delta, \pi/\Delta]$, the energy expression means that there are more than one point satisfying the linear energy-momentum relation, implying fermion doubling. Previous works [20,21] provided a solution to eliminate this effect.

Figure 2 shows our proposed discretization method, which consists of two steps. First, we discretize the whole domain using a two-dimensional lattice. The Dirac spinors are evaluated at lattice points (m,n). Second, we evaluate the Dirac equation at the center of each unit cell, $(m + \frac{1}{2}, n + \frac{1}{2})$. In the Hamiltonian, the derivatives of the Dirac spinor are approximated by

$$\partial_x\psi_{m+\frac{1}{2},n+\frac{1}{2}} = \frac{\psi_{m+1,n+1} + \psi_{m+1,n} - \psi_{m,n+1} - \psi_{m,n}}{2\Delta},$$

$$\partial_y\psi_{m+\frac{1}{2},n+\frac{1}{2}} = \frac{\psi_{m+1,n+1} + \psi_{m,n+1} - \psi_{m+1,n} - \psi_{m,n}}{2\Delta}.$$

The spinors at the unit cell centers are approximated as the average of the four spinor values from the neighboring lattice points, i.e.,

$$\psi_{m+\frac{1}{2},n+\frac{1}{2}} = \frac{1}{4}(\psi_{m+1,n+1} + \psi_{m,n+1} + \psi_{m+1,n} + \psi_{m,n}). \tag{9}$$

Using this numerical scheme, the phenomenon of fermion doubling can be eliminated.

C. Incorporation of boundary conditions and matrix representation of Dirac equation

It is worth noting that in closed systems, such as rectangles and billiards, the number of Dirac equations at unit cell centers

(denoted as M) is less than the number of total spinors at lattice points (denoted as N), i.e., $M < N$. The difference needs to be accounted for by the boundary conditions. To explain how boundary conditions are incorporated in our solution procedure, we write the Dirac equation in matrix form. In particular, we let $\Psi = (\psi_1, \psi_2, \ldots, \psi_N)^T$ be the column vector containing all spinor values on the lattice, where Ψ actually has $2N$ components. Let $D_x/(2\Delta)$, $D_y/(2\Delta)$, and $A/4$ be the matrix form of the operators ∂_x, ∂_y, and the averaging operator in Eq. (9), respectively. These matrices are all of dimension $M \times N$. In matrix form, Eq. (5) becomes

$$\left[-\frac{2i\hbar v}{\Delta}(D_x \otimes \sigma_x + D_y \otimes \sigma_y) + VA \otimes \mathbf{1}_2 \right] \Psi = EA \otimes \mathbf{1}_2\Psi. \tag{10}$$

Since we have $2M$ equations, we need $2N - 2M$ boundary conditions that can be written as

$$B\Psi = 0, \tag{11}$$

where B is a $(2N - 2M) \times 2N$ matrix. Realizing that not all spinors are independent, we permute the spinor vector by

$$\Psi' = P\Psi = \begin{bmatrix} \Psi_D \\ \Psi_B \end{bmatrix}, \tag{12}$$

where Ψ_D are independent Dirac spinors and Ψ_B are spinors at the boundary that can be expressed by other components in Ψ_D, and P is an orthogonal permutation matrix. Defining

$$H' = \left[-\frac{2i\hbar v}{\Delta}(D_x \otimes \sigma_x + D_y \otimes \sigma_y) + VA \otimes \mathbf{1}_2 \right] P^T,$$

$A' = A \otimes \mathbf{1}_2 P^T$, and $B' = BP^T$, we obtain

$$H'\Psi' = EA'\Psi', \qquad B'\Psi' = 0. \tag{13}$$

Utilizing the boundary conditions, Ψ_B can be explicitly expressed by Ψ_D. Let $B' = [B_1, B_2]$, where B_2 is a square matrix. We write

$$\Psi_B = -B_2^{-1}B_1\Psi_D.$$

Letting $H' = [H_1, H_2]$ and $A' = [A_1, A_2]$, where H_2 and A_2 are square matrices, and substituting Ψ_B into $H'\Psi' = EA'\Psi'$, we finally obtain

$$H_D\Psi_D = E\Psi_D, \tag{14}$$

where

$$H_D = \left(A_1 - A_2 B_2^{-1} B_1 \right)^{-1} \left(H_1 - H_2 B_2^{-1} B_1 \right).$$

One issue with the newly defined Hamiltonian H_D is that it is not Hermitian in general. This non-Hermitian characteristic is caused by the finite domain and lattice approximation of the original smooth boundaries. However, the eigenvalues of H_D are all real. To overcome this difficulty, we introduce

$$H = (H_D + H_D^\dagger)/2, \tag{15}$$

the Hamiltonian for a new physical system, where the difficulties associated with nonsmooth boundaries due to lattice discretization are overcome. For small values of Δ, the energy spectra of the two systems are identical, and the eigenstates of the two systems are very close to each other, especially at low energies, where the discretized system mimics the Dirac equation perfectly.

III. RESULTS

A. Solutions in analyzable geometry

To validate our method, we, first, choose a simple geometry, for which the eigenvalues and eigenstates of the Dirac equation can be calculated analytically, and compare directly the numerical results with the analytic ones. Even for very simple geometry, due to the entanglement of the two Cartesian coordinates in the Dirac equation, the problem is not analytically solvable except for certain special types of boundary conditions for which the variables can be separated. One particular class of solvable systems are those with circular boundaries, whose general solutions are

$$\psi_n = N_n e^{in\theta} \begin{bmatrix} Z_n(kr) \\ \operatorname{sgn}(E - V)ie^{i\theta}Z_{n+1}(kr) \end{bmatrix}, \quad n = 0, \pm 1, \ldots, \tag{16}$$

where $k = |E - V|/(\hbar v)$ and N_n is a normalization constant. For rings, $Z_n(x)$, the radial function of the spinor components, is a linear combination of the first- and second-kind Bessel functions, $J_n(x)$ and $Y_n(x)$. However, for circles, $Z_n(x) = J_n(x)$ because of the divergence of $Y_n(x)$ at the origin. For our analytical calculation, we consider a ring with inner and outer radii of $R_1 = 0.5$ and $R_2 = 1$, respectively. The electrical potential is set to zero, $V = 0$, for simplicity. Analytically, one can arrive at the above general solution with potential having a staircaselike profile in the radial direction but constant in the angular direction. However, one can solve the case with arbitrary potential numerically, even when the ring is not full. Setting the potential to be zero, we can find the energy levels for each angular mode through the inner and outer boundary conditions, $E_m^{(n)} = \hbar v k_m^{(n)}$, where $k_m^{(n)}$ is obtained by solving

$$\frac{[J_{n+1}(kR_1) + J_n(kR_1)][Y_{n+1}(kR_2) - Y_n(kR_2)]}{[J_{n+1}(kR_2) - J_n(kR_2)][Y_{n+1}(kR_1) + Y_n(kR_1)]} = 1. \tag{17}$$

The eigenstates can be calculated after the normalization constants $N_m^{(n)}$ are computed. Results of these analytical calculations as compared with those from numerics are shown in Fig. 3. Almost no discrepancy can be observed. As indirect evidence, the analytical energy spectrum gives statistical results (to be discussed below) identical to numerical results, as shown in Figs. 4–6 (first column) and in Fig. 7.

B. Relativistic quantum energy-level statistics and eigenstates in two-dimensional geometries

We validate our method by calculating the energy level-spacing statistics [22,23] for relativistic quantum billiards. Figures 4–6 show results of level-spacing statistics for three representative geometric domains: a relativistically integrable ring, a chaotic billiard with one geometric symmetry about the central vertical line, and the so-called Africa shaped billiard [9] without any geometrical symmetry, respectively. In relativistic quantum systems, we have a linear relation between energy level and the square root of spectral staircase $N(E)$, $E \propto \sqrt{N(E)}$, where $N(E)$ denotes the number of eigenstates between zero and energy E. To confirm that the numerical
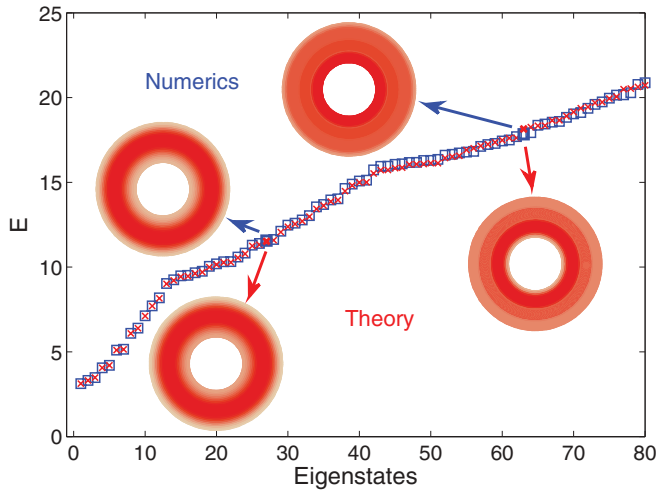
FIG. 3. (Color online) Comparison of numerical and analytical results of eigenenergies and eigenstates for the ring cavity. The lowest 80 positive eigenenergy levels and two examples of the eigenstates from numerics (blue square or above the energy spectrum) and theory (red cross or below the energy spectrum) are compared. The convenient unit convention $\hbar = v = 1$ was used in the numerical computation.

results preserve the physical properties of the system, we investigate the nearest-neighbor fluctuations of the energy spectra. For relativistically integrable quantum systems, for example, circles or rings governed by the Dirac equation, the
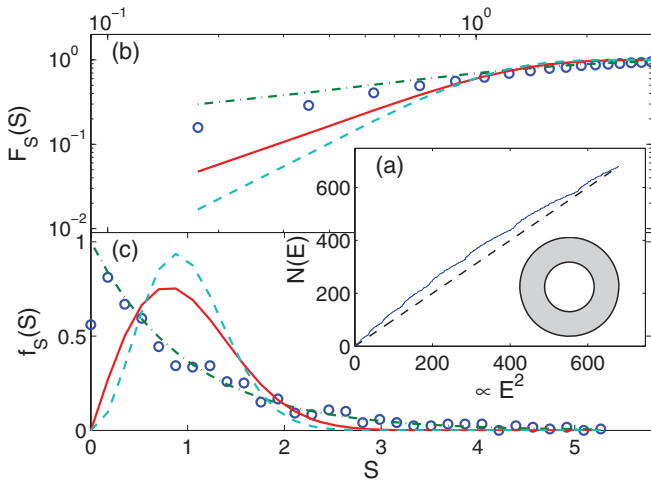

FIG. 4. (Color online) Level-spacing statistics for eigenenergies of the ring domain. Inset (a) shows spectral staircase $N(E)$ as a function of E^2. The dashed lines represent the linear relationship between $N(E)$ and E^2. Horizontal axes are linear mappings of E^2 to the range $[0,N]$, where N is the total number of eigenstates. Panel (b) is the cumulative distribution of the nearest-neighbor spacing $F_S(S)$ as a function of spectral spacings $S_n = E_{n+1}^2 - E_n^2$. Panel (c) represents the density distribution $f_S(S)$ of $F_S(S)$ in (b). In both the middle and bottom rows, green dash-dotted, red solid, and cyan dashed lines denote theoretical distribution curves for Poisson, GOE, and GUE statistics, respectively. The results of the ring are obtained through a polar coordinate version of our numerical method to preserve the perfect circular symmetry.
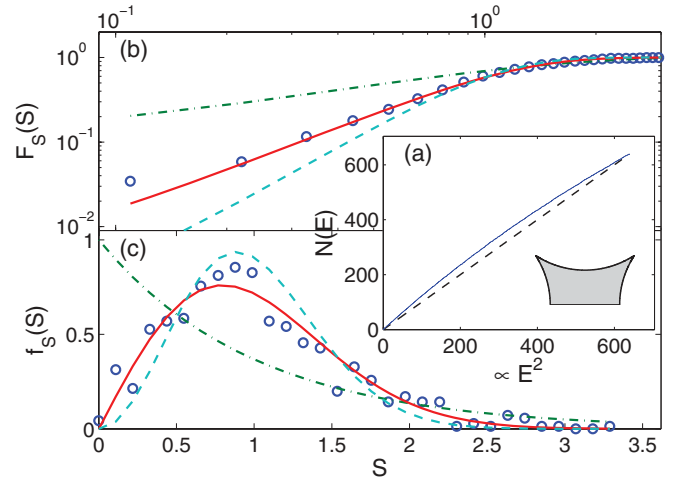

FIG. 5. (Color online) Level-spacing statistics for eigenenergies of the chaotic bow-tie domain. Figure legends are the same as for Fig. 4.

level spacing statistics should be Poisson. For nonintegrable systems, if the system preserves geometric symmetry of some kind (such as a stadium billiard), the nearest energy-level spacing statistics fall between those of Poisson and GOE (Gaussian orthogonal ensemble). In the fully chaotic case, e.g., the chaotic billiard in Figs. 5 and 6, the GOE statistics apply. However, if no geometric symmetry is present in the system, e.g., the Africa billiard, the level-spacing statistics should be those given by GUE (Gaussian unitary ensemble) according to the result of Berry and Mondragon [9].

In addition to the linear statistics, we also consider an informative least-squares statistic of the energy spectra, the spectral rigidity of the third type, Δ_3 [22,23], as a function of energy range L, where $[0,L]$ denotes the range of energy levels under consideration. Figure 7 shows the Δ_3 statistics for the three domains we considered, as well as theoretical expectation curves for Poisson, GOE, and GUE statistics, where an excellent agreement is obtained for all cases.
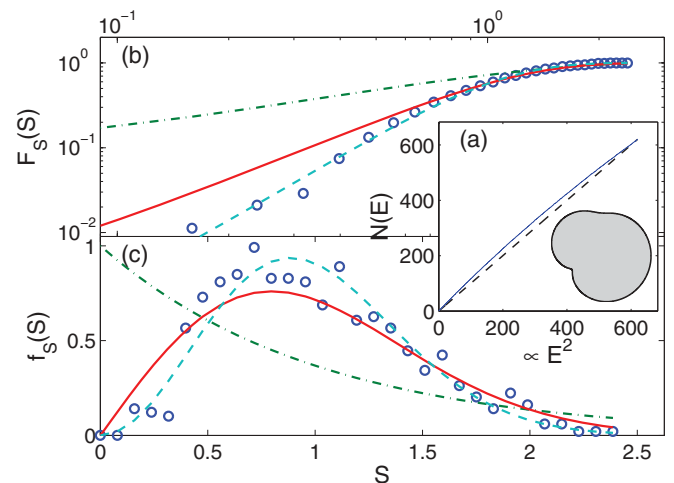

FIG. 6. (Color online) Level-spacing statistics for eigenenergies of the chaotic Africa domain. Figure legends are the same as for Fig. 4.
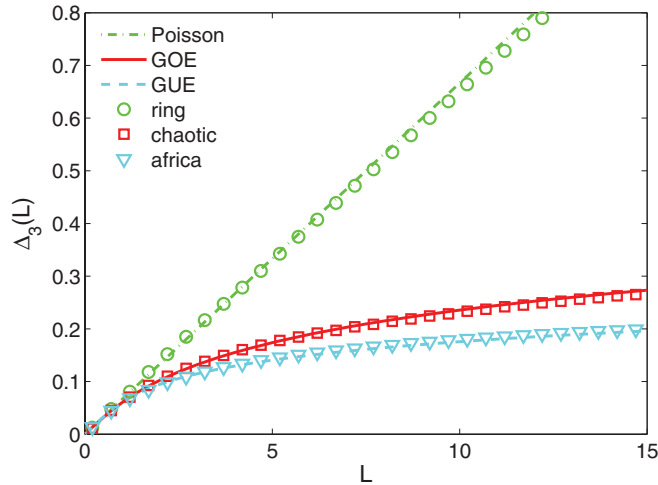
FIG. 7. (Color online) Spectral rigidity $\Delta_3(L)$ for the three domains in Figs. 4–6. Lines with different styles denote theoretical expectations of spectral rigidity for the respective statistics.

Representative eigenstates for nonintegrable billiards are shown in Fig. 8 for the bow-tie chaotic billiard and in Fig. 9 for the chaotic Africa billiard. These are examples of *truly* relativistic quantum scars from the Dirac equation. We note that quantum scars have been observed in graphene systems [7] in the regime where the energy-momentum relation is linear, but they are still solutions of the Schrödinger equation obtained by the tight-binding method. The scars shown in Figs. 8 and 9 are obtained by solving the Dirac equation which, to our knowledge, have not been reported previously.

IV. BOUNDARY CONDITIONS IN GRAPHENE SYSTEMS

Because of the high relevance of our method for solving the Dirac equation to experimental graphene systems, it is insightful to examine such systems with the kind of
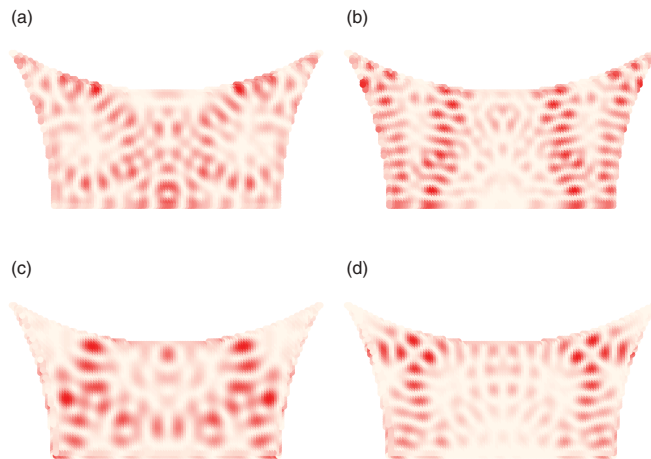

FIG. 8. (Color online) Examples of eigenstates of the Dirac equation for a bow-tie chaotic billiard. The maximum height (vertical distance from tip to base) is set to 1, and the distance between two tips is 2. Panels (a)–(d) are for $E = 36.1335, 43.0190, 27.9300,$ and 36.2729, respectively. Panels (a) and (b) show the ϕ component, while (c) and (d) show the χ component.
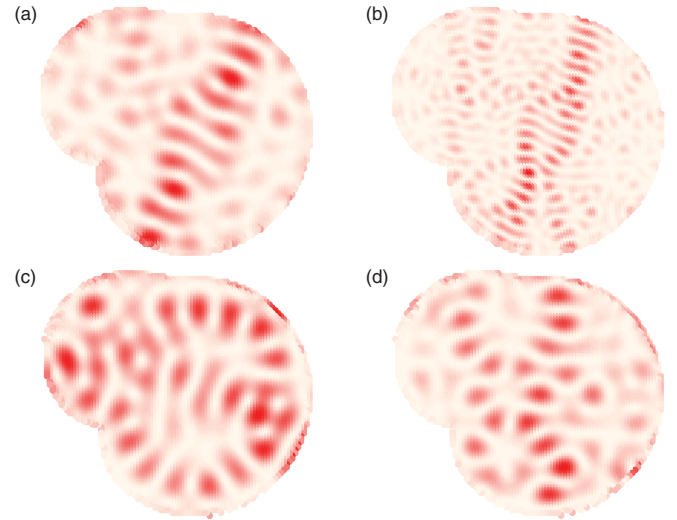

FIG. 9. (Color online) Examples of eigenstates of the Dirac equation for the chaotic Africa billiard. The domain is confined within a rectangular box $x \in [-0.99, 1.35]$ and $y \in [-1.22, 0.92]$. Panels (a)–(d) are for $E = 15.0468, 32.7638, 13.4838,$ and 15.2402, respectively. Panels (a) and (b) show the ϕ component, while (c) and (d) show the χ component.

boundary conditions treated in Ref. [12]. As explored there, graphene lattice terminated in an arbitrary orientation usually possesses complicated boundary conditions, as can be seen from Eqs. (3.8) and (3.9) in Ref. [12]. In the summation form in Eq. (3.10), only the terms with $|\lambda| = 1$ form the four-component spinor in the Dirac equation, and the rest of them describe how the boundary modes decay from the edge. By such an analysis, the authors of Ref. [12] found that, for most orientations, the boundary condition should be zigzag-like. The staggered boundary potential in graphene mimics the infinite-mass confinement for Dirac particles, leading to a boundary condition that sits on an extreme point opposite from the zigzag one. Consequently, the boundary conditions for confined Dirac particles and for the terminated graphene lattice differ somewhat.

From the point of view of symmetry, graphene system in the absence of magnetic field preserves the time-reversal symmetry, which is the starting point of Ref. [12]. The staggered lattice potential breaks the pseudospin symmetry of the sublattice, which resembles the symplectic symmetry of a spin system but preserves the true time-reversal symmetry. A unique characteristic of graphene systems is the occurrence of pseudospins. However, the Dirac equation describes the behavior of a single relativistic quantum particle, for which the phenomenon of pseudospins does not exist. As a result, for relativistic quantum systems described by the Dirac equation, the mass term (not necessarily infinite) breaks the true time-reversal symmetry. This difference can be revealed, for example, by the statistics of the energy-level spacing in the corresponding classes of classically chaotic billiards, where the graphene billiard exhibits GOE statistics, while the Dirac billiard has the GUE statistics.

Reference [12] studies the boundary conditions of a continuous Dirac-like equation for the pseudoparticles of

graphene systems, as imposed by the discrete-lattice structure of graphene. A complete description of graphene incorporating boundaries needs four-component spinors due to the presence of a pseudospin for A and B atoms in a unit cell and a pseudospin for the two nondegenerate valleys. The method we have developed to solve the 2D Dirac equation with two-component spinors thus describes the relativistic quantum motion of the graphene pseudoparticles in the absence of intervalley scatterings. Since the boundaries of graphene flakes will, in general, mix quantum dynamics associated with the two valleys, the two-component Dirac equation cannot provide a complete description of such situations. Our point is that we have developed an efficient method to solve the Dirac equation in an arbitrary shaped billiard, and the method can be used to provide deep understanding of phenomena such as scars and pointer states in quantum dots made of materials with linear energy-momentum dispersion relation such as graphene. While, in general, systems described by the Dirac equation are not identical to experimentally widely investigated quantum-dot systems, locally the dispersion relation is the same. Our method thus can be used to probe such quantum-dot systems and gain deeper insights through investigation of the Dirac billiards for the low-energy states, despite the differences in the boundary conditions between the Dirac and experimental graphene systems.

V. CONCLUSION AND DISCUSSIONS

To obtain solutions of the Dirac equation in *arbitrary* two-dimensional geometries, which includes complete sets of both eigenvalues and eigenfunctions, it is essential to address the question of whether truly relativistic quantum scars in chaotic billiards exist. Such a method is also necessary for studying

and exploring relativistic quantum behaviors and phenomena in graphene systems. We have developed a general method to address this outstanding issue. The innovative aspects of our method are a proper incorporation of the boundary conditions and an efficient discretization scheme to represent the Dirac equation in matrix form. For a classically integrable system in a circular domain for which analytic solutions of the Dirac equation are available, our method yields results that are in excellent agreement with the analytic ones. For general geometries, including those whose dynamics are chaotic in the classical limit, our method yields the correct statistics of the solutions, such as the energy level-spacing distributions.

We anticipate that our method or its variants will become a basic tool to address a host of problems arising in the study of relativistic quantum mechanics in condensed matter devices. We have focused our effort on planar system mainly because graphene is two dimensional. However, our method can be reduced straightforwardly to one-dimensional systems. Extension to three-dimensional systems is also feasible. Particularly, in three dimensions, the Dirac spinor consists of at least four components and the Dirac tensors $\boldsymbol{\alpha}$ and β should be modified accordingly. One can still use the zero outgoing current flux and a similar lattice discretization, where now the Dirac equation needs to be evaluated at the centers of unit lattice cubes.

[1] S. W. McDonald and A. N. Kaufman, Phys. Rev. Lett. **42**, 1189 (1979); Phys. Rev. A **37**, 3067 (1988).

[2] E. J. Heller, Phys. Rev. Lett. **53**, 1515 (1984).

[3] E. B. Bogomolny, Physica D **31**, 169 (1988).

[4] M. V. Berry, Proc. R. Soc. London A **423**, 219 (1989).

[5] H. J. Stöckmann, *Quantum Chaos: An Introduction* (Cambridge University Press, Cambridge, UK, 1999).

[6] K. S. Novoselov, A. K. Geim, S. V. Morozov, D. Jiang, Y. Zhang, S. V. Dubonos, I. V. Grigorieva, and A. A. Firsov, Science **306**, 666 (2004); C. Berger, Z. Song, T. Li, X. Li, A. Y. Ogbazghi, R. Feng, Z. Dai, A. N. Marchenkov, E. H. Conrad, P. N. First, and W. A. de Heer, J. Phys. Chem. B **108**, 19912 (2004); K. S. Novoselov, A. K. Geim, S. V. Morozov, D. Jiang, M. I. Katsnelson, I. V. Grigorieva, S. V. Dubonos, and A. A. Firsov, Nature **438**, 197 (2005); Y. Zhang, Y.-W. Tan, H. L. Stormer, and P. Kim, *ibid*. **438**, 201 (2005); A. H. Castro Neto, F. Guinea, N. M. R. Peres, K. S. Novoselov, and A. K. Geim, Rev. Mod. Phys. **81**, 109 (2009); N. M. R. Peres, *ibid*. **82**, 2673 (2010).

[7] L. Huang, Y.-C. Lai, D. K. Ferry, S. M. Goodnick, and R. Akis, Phys. Rev. Lett. **103**, 054101 (2009).

[8] X.-L. Qi and S.-C. Zhang, Phys. Today **63**, 33 (2010); M. Z. Hasan and C. L. Kane, Rev. Mod. Phys. **82**, 3045 (2010).

[9] M. V. Berry and R. J. Mondragon, Proc. R. Soc. London A **412**, 53 (1987).

[10] Recently, a method was developed to study the transport of Dirac fermions in *open* graphene ribbon systems. The method was based on transfer matrix, which can be used to study the transport properties through a graphene ribbon with periodic boundary conditions in the transverse direction. See J. Tworzydlo, C. W. Groth, and C. W. J. Beenakker, Phys. Rev. B **78**, 235438 (2008).

[11] S. Das Sarma, S. Adam, E. H. Hwang, and E. Rossi, Rev. Mod. Phys. **83**, 407 (2011).

[12] Boundary conditions are also an important issue in graphene systems, e.g., with respect to armchair or zigzag boundaries. See, for example, A. R. Akhmerov and C. W. J. Beenakker, Phys. Rev. B **77**, 085423 (2008).

[13] V. Alonso and S. Vincenzo, J. Phys. A: Math. Gen. **30**, 8573 (1997).

[14] P. Alberto, C. Fiolhais, and V. M. S. Gil, Eur. J. Phys. **17**, 19 (1996).

[15] V. Alonso, S. D. Vincenzo, and L. Mondino, Eur. J. Phys. **18**, 315 (1997).

[16] A. Chodos, R. L. Jaffe, K. Johnson, C. B. Thorn, and V. F. Weisskopf, Phys. Rev. D **9**, 3471 (1974).

[17] A. Chodos, R. L. Jaffe, K. Johnson, and C. B. Thorn, Phys. Rev. D **10**, 2599 (1974).

[18] A. W. Thomas, Adv. Nucl. Phys. **13**, 1 (1984).

[19] For example, M. E. Peskin and D. V. Schroeder, *An Introduction to Quantum Field Theory* (Westview Press, Boulder, CO, 1995), Chap. 3.

[20] R. Stacey, Phys. Rev. D **26**, 468 (1982).

[21] C. M. Bender, K. A. Milton, and D. H. Sharp, Phys. Rev. Lett. **51**, 1815 (1983).

[22] F. Haake, *Quantum Signatures of Chaos*, 2nd ed. (Springer, Berlin, 2001).

[23] F. J. Dyson and M. L. Mehta, J. Math. Phys. **4**, 701 (1963); O. Bohigas and M. J. Giannoni, Ann. Phys. **89**, 393 (1975); O. Bohigas and M.-J. Giannoni, In *Mathematical and Computational Methods in Nuclear Physics*, Lecture Notes in Physics, Vol. 209 (Springer, Berlin, 1984); O. Bohigas, M.-J. Giannoni, and C. Schmit, Phys. Rev. Lett. **52**, 1 (1984); M. V. Berry, Proc. R. Soc. London A **400**, 229 (1985); U. Stoffregen, J. Stein, H.-J. Stöckmann, M. Kuś, and F. Haake, Phys. Rev. Lett. **74**, 2666 (1995); P. So, S. M. Anlage, E. Ott, and R. N. Oerter, *ibid.* **74**, 2662 (1995); L. Huang, Y.-C. Lai, and C. Grebogi, Phys. Rev. E **81**, 055203(R) (2010); Chaos **21**, 013102 (2011).